PARAMETERS CONTROLLING ROUGHNESS EFFECTS IN A SEPARATING BOUNDARY LAYER

Carolyn D. Aubertine, John K. Eaton
Department of Mechanical Engineering, Stanford University
Stanford, California 94305-3030, USA
caubertine@stanford.edu, eaton@vonkarman.stanford.edu

Simon Song
Sandia National Laboratory
Livermore, California 94551-9951, USA
ssong@sandia.gov

ABSTRACT

The effects of wall roughness were examined experimentally for two different rough-wall cases involving flow over a ramp with separation and reattachment. For these cases, the roughness Reynolds number was matched at two different momentum thickness Reynolds numbers. Both flow conditions were fully rough. The effect of increasing the wall roughness was to increase the friction velocity and increase the separation region size. The two rough-wall cases produced different size separation regions and different friction velocity values. In both cases, the outer layer turbulence was mainly affected by the change in the friction velocity.

INTRODUCTION

While many laboratory experiments are performed over smooth surfaces, practical surfaces are often rough. This is especially true for large-scale vehicles that operate at very high Reynolds numbers. As the viscous length scale decreases with increasing Reynolds number, the roughness height becomes more important. At high Reynolds numbers, all but extremely smooth surfaces are hydrodynamically rough. The effect of the roughness is to increase the skin friction, and thus the boundary layer momentum deficit. This may affect separation behavior, and thereby overall vehicle performance.

The effects of roughness have been studied extensively for pipe flows and flat plate boundary layers. A recent review of roughness research performed in zero pressure gradient boundary layers by Raupauch et al. (1991) examined both atmospheric and laboratory flows. The type of roughness varied and included meshes, screens and perforated plates (Krogstad & Antonia 1999, Perry et al 1987, Tachie et al 2000), uniform spheres (Ligrani & Moffat 1986), grooves of a variety of dimensions (Bandyopadhyay 1987, Keirsbulck et al 2002, Perry et al 1969) wavy machined surfaces (Perry et al 1987), uniform sandgrains (Bandyopadhyay 1987, Bergstrom et al 2002, Tachie et al 2000) and sandpaper (Song & Eaton 2002a). In general, for each new roughness geometry, it is necessary to determine the effective roughness height and the virtual origin of the boundary layer. Thus far, no theory is available to predict these quantities given only a geometric specification of the roughness.

Roughness is often characterized based on how it affects the flat plate mean velocity profile, which may be matched to a modified log law as:

$$\frac{U}{U_\tau} = \frac{1}{\kappa}\ln\left(\frac{yU_\tau}{\nu}\right) + B - \Delta\frac{U}{U_\tau} \qquad (1)$$

where k and B are standard log-law constants and y is measured from a virtual origin located somewhere above the base level of the roughness (Ligrani & Moffat 1986, Perry et al 1969). The last term is called the roughness function, and shifts the velocity profile down in a standard law of the wall plot. Matching the velocity profile to this form is difficult because both the friction velocity and the y-origin shift are unknown. Various methods of fitting the velocity profile (Krogstad & Antonia 1999, Perry et al 1987, Tachie et al 2000), a momentum integral analysis (Ligrani & Moffat 1986) and extrapolation of the total shear stress (Song & Eaton 2002a) have all been used to determine the friction velocity. None of these techniques is entirely satisfactory, and in the absence of direct shear force measurements, the uncertainty in U_τ is fairly large. In recent work, Smalley et al. (2002) have questioned the utility of characterizing roughness effects based solely on mean velocity measurements.

Boundary layers are divided into smooth, transitionally rough and fully rough regimes, based on the roughness Reynolds number, which is the ratio of the roughness height to the viscous length scale. For smooth boundary layers, the roughness Reynolds number is less than 5 to 10 and for fully rough boundary layers the roughness Reynolds number is greater than 55 to 90. Ligrani & Moffat (1986) used an equivalent sandgrain roughness k_s, rather than k, for these limits. This equivalent sandgrain height relates the actual roughness height to the uniform sandgrain size used in Nikuradse's

experiments for pipe flows, giving the same value of the roughness function ($\Delta U/U_\tau$). Some of the previous work implies then that roughness effects are fully determined by the roughness Reynolds number, although there is no work showing that roughness effects are independent of other geometric scales such as the roughness height divided by the boundary layer thickness.

Another open question is the effect the roughness has on both the mean velocity and turbulent stresses far away from the wall. The idea of wall similarity was proposed by Raupauch et al. (1991) who observed that far from the wall, the roughness has no effect on the flow other than to change U_τ. Keirsbulck et al. (2002) confirmed this result and demonstrated that the normalized stresses collapse outside the roughness sublayer. He also noted that in the inner layer, stresses depend strongly on the roughness. Ligrani & Moffat (1986) noted that the streamwise normal stress was invariant in the outer region when scaled on the friction velocity, while the inner region was invariant only for fully rough flows. Krogstad et al. (1992) noticed a departure of the rough-wall profiles from the smooth-wall profiles over a significant portion of the boundary layer. Bergstrom et al. (2002) also noted a deviation in the mean velocity profiles outside the inner region of the boundary layer. Tachie et al. (2000) noted that the mean velocity profile changed and that the outer peaks in the turbulence profiles flattened out for the rough case

Few studies have focused on the effects of roughness on a separating flow. For a laminar boundary layer it is well known that roughness delays the separation point by triggering transition. Recent work by Durbin et al. (2001) and Song & Eaton (2002a) showed that separation was very sensitive to upstream roughness, probably due to the increased velocity deficit making the boundary layer less resistant to separation.

The present work attempts to cast light on some of the open questions about roughness effects by independently varying the roughness Reynolds number and the ratio of the roughness height to the boundary layer thickness, k/δ_{99}. The work extends the work of Song & Eaton (2002a) who examined a rough wall boundary layer that developed on a flat plate then separated as it flowed down a contoured ramp. Both smooth and rough-wall data have been acquired at two different momentum thickness Reynolds numbers by varying the ambient pressure in the wind tunnel. The roughness size was chosen to maintain the roughness Reynolds number at a constant value, while allowing k/δ_{99} to vary by a factor of four.

EXPERIMENTS

The experiments were performed in a closed loop wind tunnel, which is mounted inside a pressure vessel. The measurements were made with a two component, high-resolution laser Doppler anemometer (LDA) described by DeGraaff & Eaton (2001). The wind tunnel test section has a rectangular cross section and is 152 mm by 711 mm by 2.9 m in length. The flow geometry is shown in Figure 1. The boundary layer is tripped 150 mm downstream of a 5:1 contraction and develops over a 1.6 m long flat plate. The flow is then mildly contracted over 169 mm on the bottom wall, which reduces the test section height from 152 mm to 131 mm. The boundary layer then relaxes to equilibrium characteristics on a 320 mm long flat plate. At a typical freestream velocity of 15 m/s, the freestream turbulence level is approximately 0.2%.

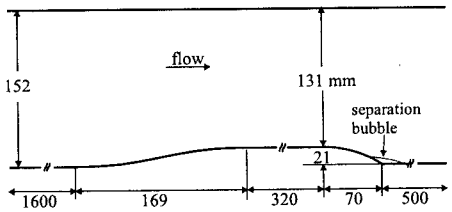

Figure 1. Flow Geometry (not to scale)

The current flow geometry consists of part of the 320 mm flat plate and a smoothly contoured ramp. The ramp has a circular arc with a radius of 127 mm. The ramp expands the tunnel height from 131 mm to 152 mm. Under smooth-wall conditions there is a separation bubble approximately centered on the ramp's trailing edge, which is 43 mm long. This geometry avoids fixing the separation point on a sharp corner so that, as in many real flows, the separation point occurs on a continuous surface, rather than at a sharp corner.

The custom LDA has a measurement volume 35 μm in diameter and 60 μm in length. Due to its small measurement volume, two of the major uncertainty sources – velocity gradient bias and two-component coincidence are eliminated. The details, including the LDA bias correction, are found in DeGraaff & Eaton (2001). Uncertainties for U, u'u', v'v', u'v' are estimated, using 5000 samples, as 1.5%, 4%, 8% and 10% of their local value respectively in the center of the profiles. Near-wall and freestream uncertainties are higher due to the local values approaching zero. Uncertainties are estimated taking into account the statistical uncertainty (5000 samples) and uncertainties in LDA fringe spacing, data filtering, and velocity bias correction

For the rough-wall measurements, two different sandpaper grits were used to establish the two conditions. For the original experiments, 36 grit sandpaper (Norton P36D) was used; for the new work, 120 grit sandpaper (Norton P120CF) was used. The sandpaper was applied from 1.3 m upstream of the ramp to the ramp trailing edge. Control experiments were performed using smooth paper to show that the elevation of the wall position due to the sandpaper thickness has no influence on the flow.

A characteristic height chosen as the average of the local crest heights; k_{ave} was measured for each case. This average local crest height was determined at a number of locations on a sheet of sandpaper using an optical microscope. The measurements were made by bringing into focus the top peak of a sandgrain, recording its relative height based on the microscope's focus

Case	Symbol	U_∞ (m/s)	$P_{ambient}$	k_{ave} (mm)	Re_k	Re_{ks}	$Re_{\theta,ref}$	δ_{99} (mm)	θ (mm)	k_s (mm)	$\Delta U/U_\tau$
1	□	20.2	1 atm	-	-	-	3400	27.2	2.61	-	-
2	■	20.3	4 atm	-	-	-	13200	26.5	2.21	-	-
3	○	20.1	1 atm	0.52	42	210	3900	25.2	3.03	2.6	9.91
4	●	19.2	4 atm	0.13	39	210	16600	27.7	2.84	0.7	9.58

Table 1. Cases Examined and Roughness Parameters

setting, and then bringing into focus the paper surface and recording its relative height in the same manner. The difference in these relative heights was considered to be the characteristic height of that grain. These results were then compared with the sandgrain sizes used in the production of the sandpaper, as reported by the manufacturer, and found to match within the uncertainty of the measurements. For the 36 grit sandpaper, the value of k_{ave} was 0.52 mm with a standard deviation of 0.05 mm. This value for the average local crest height is much different than the one reported in Song & Eaton (2002a), due to a difference in measurement technique. The previous technique used a caliper, which preferentially measured the highest peaks on the sandpaper. The optical technique allowed for a more distributed measurement of peak height and avoided preferentially measuring the largest grains. For the 120 grit sandpaper, the value of k_{ave} was 0.13 mm with a standard deviation of 0.01 mm.

RESULTS

The results are presented in a Cartesian coordinate system with x being parallel to the upstream flow and y maintained normal to x, even over the curved ramp surface. The normalized coordinate x' denotes a streamwise location normalized with the ramp length, with the origin at the beginning of the ramp. In some plots, the y coordinate is normalized by the ramp height, h = 21 mm. Measurements were acquired for four different cases as indicated in Table 1. The two smooth wall cases were run at one and four atmospheres ambient pressure with freestream velocities near 20 m/s. The increase in pressure from one to four atmospheres produced just under a four-fold increase in the momentum thickness Reynolds number. The two rough wall cases also were run at one and four atmospheres ambient pressure, again producing approximately a four-fold increase in Re_θ. The roughness heights were chosen to match the roughness height Reynolds number between the two cases. The freestream velocity was lowered to 19.2 m/s for the four-atmosphere case to precisely match the roughness Reynolds number.

Flat plate data were measured at x' = -2.00, well upstream of any pressure gradient induced by the ramp. Mean velocity profiles at this location are shown in Figure 2 for all four cases. Overall parameters describing these profiles are shown in Table 1. All four boundary layers have roughly the same overall thickness with δ_{99} values ranging from 25.2 to 27.7 mm. The roughness produces the expected downward shift in the law of the wall plot. The roughness function ($\Delta U/U_\tau$) is approximately equal for the two cases. The equivalent sand grain roughness is k_s = 2.6 mm for the one atmosphere case and k_s = 0.7 mm for the four-atmosphere case. These values are approximately five times greater than the actual measured roughness heights. The roughness Reynolds number evaluated using the equivalent sand grain roughness $U_\tau k_s/\nu$ was 210 for both cases, placing them well within the fully rough regime.

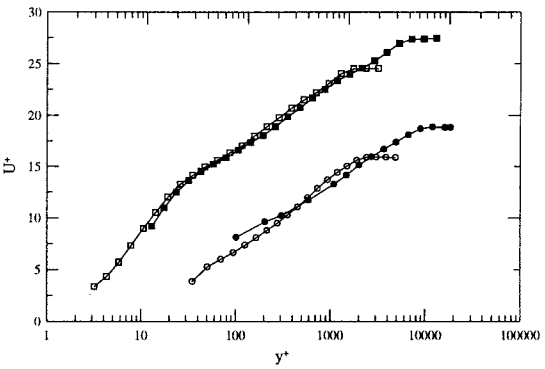

Figure 2. Law of the Wall

The flat plate velocity profiles are plotted as normalized velocity deficit vs. y/δ_{99} in Figure 3. All four profiles are in fairly close agreement for $y/\delta_{99} > 0.06$, especially considering the fairly large uncertainty in the friction velocity for the rough wall cases. A similar collapse of the profiles was observed using the scaling for vertical height proposed by Clauser (1956), $yU_\tau/\delta_{99}U_e$. The Reynolds stress profiles for the flat plate are shown in Figure 4, where the mixed scaling proposed by DeGraaff & Eaton (2000) for smooth wall flows has been used. The wall normal coordinate is normalized by the boundary layer thickness to examine the outer layer behavior. Generally, the stresses collapse fairly well for $y/\delta_{99} > 0.1$, although the shear stress data appear fairly noisy. Overall, the mean velocity and turbulence measurements show that the boundary layer structure outside of $y/\delta_{99} = 0.1$ is only affected by the roughness insofar as the roughness changes the friction velocity. This conclusion is opposite of that reached by Krogstad & Antonia (1999). This disagreement may be due to differences in the roughness types studied.

Two types of measurements were made in the downstream flow to assess the importance of the roughness on flow separation. First, the separation and reattachment points were located, then profiles of the mean velocity and Reynolds stresses were measured for each case at the separation and reattachment points, and at x' = 0.00 and 1.00. For the smooth-wall case, the separation point was found by scanning in the

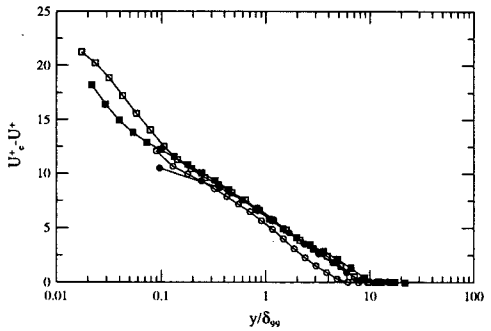

Figure 3. Mean Deficit Profile

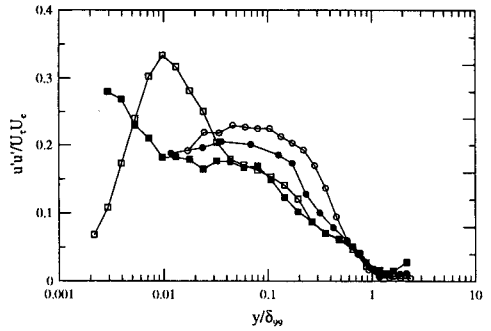

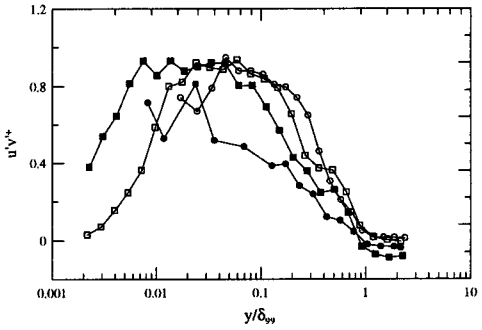

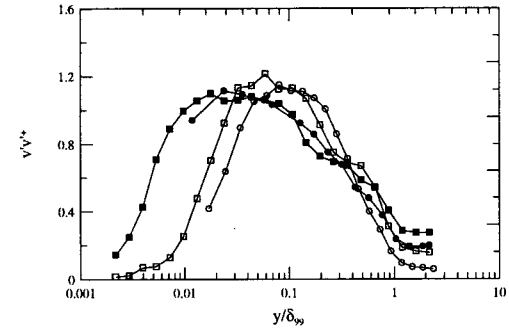

Figure 4. Reynolds stresses in the upstream boundary layer

streamwise direction at a height of 60 μm above the ramp. Measurements were made every millimeter in the streamwise direction until the separation point was located. For the rough-wall cases, the same technique was employed, however, for the one-atmosphere rough-wall case, the maximum scanning height was 800 μm, while for the four-atmosphere case, the maximum height was 100 μm. The separation point was taken to be the point of zero mean velocity. The reattachment points were found in a similar way, for all cases the wall was smooth and flat, so the location of these points is known with the same accuracy for all cases.

The separation and reattachment location measurements are summarized in Table 2. The two smooth-wall cases were essentially identical, indicating that there is no significant effect of Reynolds number on the separation bubble. The same separation point was found for the one atmosphere rough wall case, but this measurement is highly uncertain due to the difficulty in making near wall measurements with the large roughness elements. Other velocity profiles indicated that separation occurred farther upstream as shown by Song & Eaton (2002a). The reattachment point moved downstream to x' = 1.76 vs. x' = 1.36 for the smooth wall case. Thus, the separation bubble length increased by at least 65% for this case. The separation point was easier to measure for the high Reynolds number rough wall case. It was observed to move upstream to x' = 0.62. The reattachment point moved to x' = 1.60. In other words, the separation bubble for the high Reynolds number rough case is significantly larger than for the smooth wall cases, but significantly shorter than for the low Reynolds number rough wall case.

Case	Separation Point	Reattachment Point
1	0.74	1.36
2	0.74	1.39
3	0.74	1.76
4	0.62	1.60

Table 2. Separation and Reattachment Points

The measured mean velocity profiles for all four cases are shown in Figure 5. The measurements are normalized by the freestream velocity at x' = -2.00. The larger separation bubbles for the rough wall cases are apparent. Also interesting to note are the differences in the upstream mean velocity profiles using this scaling. While the overall boundary layer thickness is nearly the same for all four cases, it is clear that the velocity deficit is much greater in the middle of the boundary layer for the rough cases. This is especially true for the one atmosphere rough- wall case, which produces the largest separation bubble.

The development of the wall normal Reynolds stress is seen in Figure 6. This stress is typical of all three measured stress components. The stress is scaled on the friction velocity at the reference location. The stresses are much larger for the four-atmosphere cases than for the one-atmosphere cases. Overall, the roughness has a similar impact on the Reynolds stresses for both conditions. The adverse pressure gradient of the ramp has less impact on the boundary layer, due to the enhanced mixing for the rough case. The smooth boundary layers develop strong peaks in the Reynolds stresses at the start of the adverse pressure gradient, which then move outward along the ramp. The rough-wall cases develop peaks in the stresses as well,

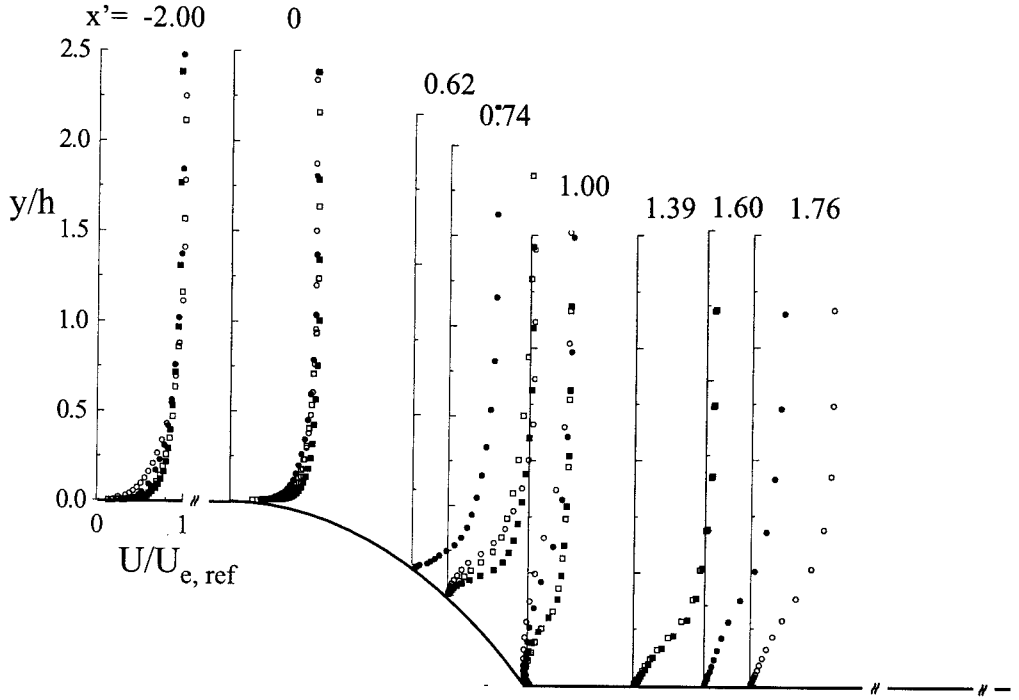

Figure 5. Mean Velocity Development

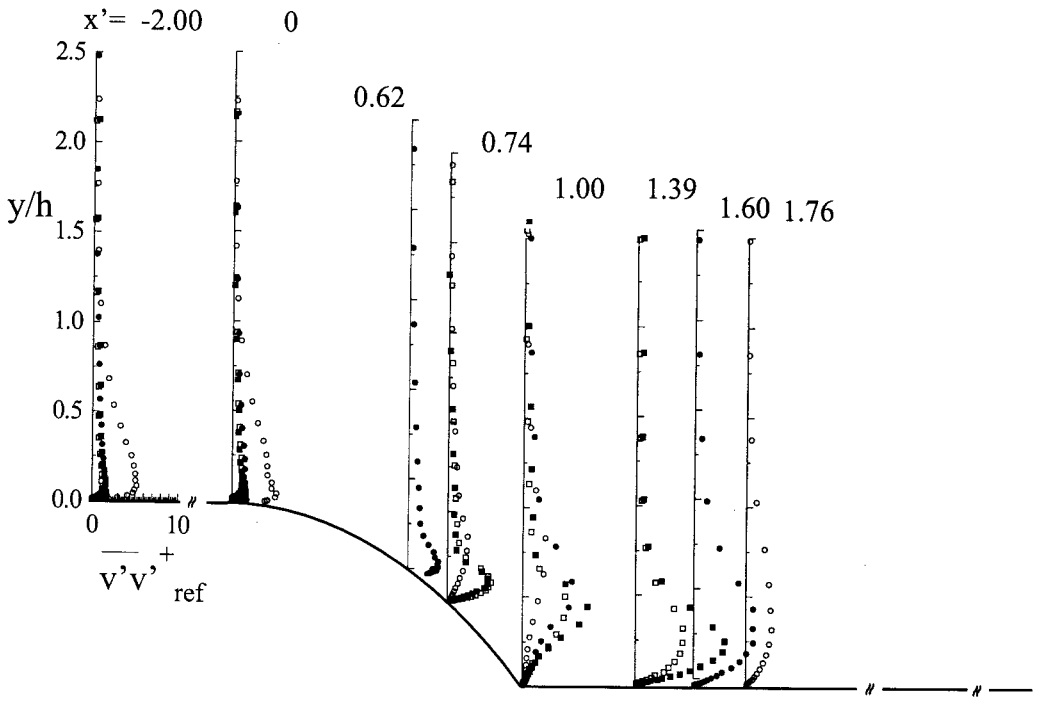

Figure 6. Reynolds stress development

but these peaks are weaker and are located farther away from the wall over the ramp.

The wall normal Reynolds stress at the reattachment point is shown in Figure 7. The stress is normalized by the mean velocity on the flat plate and the vertical height is normalized by the height of the inflection point in the mean profile. The peak stress levels and the peak heights appear to collapse well between the cases for the

same momentum thickness Reynolds number, with those run at the higher momentum thickness Reynolds number being higher than those run at the lower Reynolds number. Similar results are observed at the separation point. Song & Eaton (2002a) showed that the peaks in stresses collapse between the rough and smooth cases at each momentum thickness Reynolds number in this scaling. Since the roughness Reynolds number approaches zero, this shows that the separated shear layer is not affected by the wall conditions.

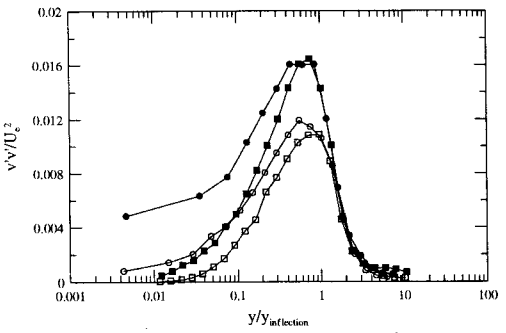

Figure 7. Reynolds stresses at reattachment

CONCLUSIONS

The effects of wall roughness were examined experimentally for two different rough-wall cases over a flat plate boundary layer with separation and reattachment. The roughness Reynolds number was matched at two different momentum thickness Reynolds numbers to examine the effect of k/δ_{99} on the flow.

When scaled by the friction velocity, the measured Reynolds stress components are seen to be unaffected by the wall roughness within their uncertainty; this is similar to previous observations by Song & Eaton (2002a). This result contrasts with the work of Krogstad & Antonia (1999) and the difference is probably due to the different characteristics of the roughness elements.

In the separated region, the rough and smooth-wall cases behaved quite differently. For the smooth-wall cases, it has been seen that the separation bubble remains the same size for different momentum thickness Reynolds numbers (Song & Eaton 2002b). The roughness produced a larger separation bubble for both momentum thickness Reynolds numbers but the increase in the size of the bubble was not the same for the two cases. This suggests that another parameter involving the ratio of the boundary layer thickness to the roughness height may be important in the determination of the size of the separation bubble. The roughness acts to increase the momentum deficit in the flat plate, which also affects the separation location and the separation bubble size. The Reynolds stresses normalized by the flat plate friction velocity squared are less sensitive to the adverse pressure gradient for the rough wall than for the smooth wall.

REFERENCES

Bandyopadhyay P. 1987. Rough-wall turbulent boundary layers in the transition regime. *Journal of Fluid Mechanics* 180: 231-66

Bergstrom D, Kotey N, Tachie M. 2002. The effects of surface roughness on the mean velocity profile in a turbulent boundary layer. *Journal of Fluids Engineering* 124: 664-70

Clauser F. 1956. The turbulent boundary layer. *Advances in Applied Mechanics* 4: 1-51

DeGraaff D, Eaton J. 2001. A high resolution laser Doppler anemometer: design, qualification, and uncertainty. *Experiments in Fluids* 20: 522-30

DeGraaff D, Eaton J. 2000. Reynolds number scaling of the flat plate turbulent boundary layer. *Journal of Fluid Mechanics* 422: 319-46

Durbin P, Medic G, Seo J-M, Eaton J, Song S. 2001. Rough wall modification of two-layer k-ε. *Journal of Fluids Engineering* 123: 16-21

Keirsbulck L, Labraga L, Mazouz A, Tournier C. 2002. Surface roughness effects on turbulent boundary layer structures. *Journal of Fluids Engineering* 124: 127-35

Krogstad P, Antonia R. 1999. Surface roughness effects in turbulent boundary layers. *Experiments in Fluids* 27: 450-60

Krogstad P, Antonia R, Browne L. 1992. Comparison between rough- and smooth-wall turbulent boundary layers. *Journal of Fluid Mechanics* 245: 599-617

Ligrani P, Moffat R. 1986. Structure of transitionally rough and fully rough turbulent boundary layers. *Journal of Fluid Mechanics* 162: 69-98

Perry A, Lim K, Henbest S. 1987. An experimental study of the turbulence structure in smooth- and rough-wall boundary layers. *Journal of Fluid Mechanics* 177: 437-66

Perry A, Schofield W, Joubert P. 1969. Rough wall turbulent boundary layers. *Journal of Fluid Mechanics* 37: 383-413

Raupauch M, Antonia R, Rajagopalan S. 1991. Rough-wall turbulent boundary layers. *Applied Mechanics Review* 44: 1-25

Smalley R, Leonardi S, Antonia R, Djenidi L, Orlandi P. 2002. Reynolds stress anisotrophy of turbulent rough wall layers. *Experiments in Fluids* 33: 31-7

Song S, Eaton J. 2002a. The effects of wall roughness on the separated flow over a smoothly contoured ramp. *Experiments in Fluids* 33: 38-46

Song S, Eaton J. 2002b. "Reynolds number effects on turbulent boundary layer with separation, reattachment, and recovery". TSD Report 146 Stanford University, Stanford, CA.

Tachie M, Bergstrom D, Balachandar R. 2000. Rough wall turbulent boundary layers in shallow open channel flow. *Journal of Fluids Engineering* 122: 533-41